General Treatment of Klystron Resonant Cavities*

KAZUO FUJISAWA†

Summary—Klystron resonant cavities are treated for general cases and their equivalent circuits are theoretically determined, which allows a fairly accurate estimate of resonant properties. It is shown that a reentrant cavity is expressed as a low-frequency series LCR_{se} circuit or a shunt LCR_{sh} circuit, taking L as the inductance of a toroidal coil with one turn and with a cross section the same as the cavity, C as the gap capacitance plus the equivalent capacitance of the cavity, and R_{se} or R_{sh} as the equivalent series or shunt resistance of the cavity at resonance. The introduction of the equivalent cavity capacitance has proved to be very effective.

The formulas derived here enable one to calculate the resonant frequency within an error of a few per cent and the shunt resistance and the Q within an error of several tenths of a per cent in most cases, and thus should prove to be very useful to the designer of microwave circuits.

Introduction

SO FAR, there has been no general theory on klystron resonant cavities of the reentrant type, so that their shapes and dimensions were mainly determined by cut-and-try method. There is an empirical statement[1] that the reentrant cavity is expressed as a low-frequency shunt LC circuit, taking L as the inductance of a toroidal coil with one turn and with the same cross section as the cavity, and C as the gap capacitance formed by plane parallel plates. The accuracy of this empirical statement is insufficient to rely upon for designing. It is said that the error of the resonant frequency exceeds 20 per cent.

As for the reentrant coaxial cavity with a toroidal rectangular cross section, there have been many works initiated by Hansen, and now we can utilize various charts to obtain its resonant frequency.[2–4] The unloaded Q and the shunt resistance of this type of cavity are also calculated and tabulated in some cases,[5] and are studied in detail by Ginzton and Nalos.[6]

However, in practice, the purely coaxial reentrant cavity is seldom used, so we need some more general calculating methods in order to design practical klystron cavities.

In this paper, an arbitrary reentrant cavity is generally treated using the theory of Green's functions. The formula for the input admittance at the gap is derived, and then its low-frequency equivalent circuit is determined in general form. Thus we can estimate its resonant properties with considerable accuracy and determine its dimensions at least in the earlier stages of designing.

The low-frequency equivalent circuit derived here theoretically has proved to be almost the same as the above mentioned empirical circuit, except for the addition of an equivalent capacitance of the cavity to the gap capacitance. By the introduction of this cavity capacitance, the accuracy of the equivalent circuit is much improved. By means of this method the error of the resonant frequency is ordinarily within a few per cent in its region of validity. The region of applicability of this equivalent circuit is estimated by comparisons with experiments and with other calculated results on the coaxial reentrant cavity.

Also, for the special reentrant cavity with an aperture gap, equivalent circuit parameters are given here with considerable accuracy.

General Theory of a Reentrant Cavity

In this Section, a reentrant cavity is generally treated, and the general expression for its input admittance at the gap is derived.

In Fig. 1, the cross section of a reentrant cavity is shown, and the cylindrical coordinates r, ϕ, and z are used as shown. In this cavity, the fundamental E-type mode with axial symmetry is excited and its field components are given by

$$E_z = \frac{1}{j\omega\epsilon_0}\frac{1}{r}\frac{\partial u}{\partial r}, \quad E_r = -\frac{1}{j\omega\epsilon_0}\frac{1}{r}\frac{\partial u}{\partial z}, \quad u = rH_\phi, \tag{1}$$

where mks units are used. u satisfies the following wave equation

$$\frac{\partial}{\partial r}\left(\frac{1}{r}\frac{\partial u}{\partial r}\right)+\frac{\partial}{\partial z}\left(\frac{1}{r}\frac{\partial u}{\partial z}\right)+\frac{k^2}{r}u \equiv L(u)+\frac{k^2}{r}u = 0, \tag{2}$$

under the boundary condition

$$\text{on } c_1 \quad \frac{\partial u}{\partial n} = 0, \tag{3}$$

where c_1 is the wall part of the boundary c of D, D being the hatched region of the cavity cross section, and $k^2 = \omega^2\epsilon_0\mu_0$.

* Manuscript received by the PGMTT, July 3, 1957; revised manuscript received, May 2, 1958.

† Dept. of Elec. Eng., Kobe Univ., Nagata, Kobe, Japan.

[1] F. E. Terman, "Radio Engineer's Handbook," McGraw-Hill Book Co., Inc., New York, N. Y., p. 263; 1943.

[2] A. E. Harrison, "Klystron Tubes," McGraw-Hill Book Co., Inc., New York, N. Y., pp. 253–262; 1947.

[3] T. Moreno, "Microwave Transmission Design Data," McGraw-Hill Book Co., Inc., New York, N. Y., pp. 230–238; 1948.

[4] D. R. Hamilton, J. K. Knipp, and J. B. H. Kuper, "Klystrons and Microwave Triodes," McGraw-Hill Book Co., Inc., New York, N. Y., pp. 73–75; 1948.

[5] *Ibid.*, pp. 77–79.

[6] E. L. Ginzton and E. J. Nalos, "Shunt impedance of klystron cavities," IRE TRANS. ON MICROWAVE THEORY AND TECHNIQUES, vol. MTT-3, pp. 4–7; October, 1955.

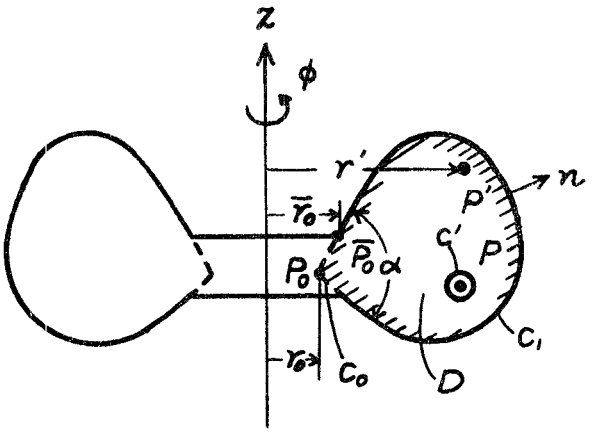

Fig. 1—Cross section of a reentrant cavity.

To solve this boundary-value problem, let us introduce Green's function $G(P, P'; k^2)$ for two points P and P' in D, which has the following properties.[7,8]

1) G, regarded as a function of P', satisfies the wave equation

$$L'(G) + \frac{k^2}{r'} G = 0, \tag{4}$$

everywhere in D except at P. The dashed symbols all refer to the point P' throughout this paper.

2) When P' is on c

$$\frac{\partial G}{\partial n'} = 0, \tag{5}$$

where n' is the outward normal to D at P'.

3) When the distance $PP' \simeq 0$ and P lies in D, G is written

$$G(P, P'; k^2) = -\frac{r'}{2\pi} \ln PP' + g(P, P'; k^2), \tag{6}$$

where g is a regular function everywhere in D. So, taking c' as an infinitesimal circle aroung P, we have

$$\oint_{c'} \frac{\partial G}{\partial n'} \frac{ds'}{r'} = 1, \tag{7}$$

where n' is the inward normal to c', and ds' is the increment of length along c'.

For a point P on the boundary c, G may be written

$$G(P, P'; k^2) = -\frac{r'}{\alpha} \ln PP' + g(P, P'; k^2), \tag{8}$$

where α is the angle subtended by c at P. The rigorous proof of this equation may be difficult, but we can confirm it by several examples.[9] Assuming (8) and taking now c' as the part in D of an infinitesimal circle around P, (7) remains valid.

4) If we denote the ith eigenvalue of the boundary-value problem, (4) and (5), as k_i, and the ith normalized eigenfunction as v_i, the following relations exist:

$$\int_D v_i(P')v_j(P') \frac{dS'}{r'} = \begin{cases} 0, & \text{if } i \neq j, \\ 1, & \text{if } i = j, \end{cases} \tag{9}$$

$$i, j = 0, 1, 2, \cdots,$$

where dS' is the increment of area at P'. Particularly, for $i = 0$

$$\left.\begin{aligned} k_i &= k_0 = 0, \\ v_i^2 &= v_0^2 = \text{const} = \frac{1}{\int_D dS'/r'} \end{aligned}\right\}. \tag{10}$$

Using these eigenvalues and eigenfunctions, G is expanded as

$$G(P, P'; k^2) = \sum_{i=0}^{\infty} \frac{v_i(P)v_i(P')}{k_i^2 - k^2}. \tag{11}$$

Then, by Green's theorem, we have

$$u(P) = rH_\phi(P) = j\omega\epsilon_0 \int_{c_0} G(P, P'; k^2)\boldsymbol{E}' \cdot d\boldsymbol{s}', \tag{12}$$

where the line integral is taken counter-clockwise around D, on the boundary section c_0 in the gap region, and $\boldsymbol{E}'$ is the electric field at P' on c_0.

Now, for simplicity, let us consider the case when the unit gap voltage is applied; then we have

$$\int_{c_0} \boldsymbol{E}' \cdot d\boldsymbol{s}' = -1. \tag{13}$$

Thence, the input admittance of the cavity at the gap edge $\bar{P}_0$ is given by

$$\begin{aligned} \vec{Y}(\bar{P}_0) &= -2\pi u(\bar{P}_0) \\ &= -j\omega\epsilon_0 2\pi \int_{c_0} G(\bar{P}_0, P'; k^2)\boldsymbol{E}' \cdot d\boldsymbol{s}'. \end{aligned} \tag{14}$$

Let us consider here how to take the cavity cross section D for the ease of practical applications. At a glance, one is liable to take D as shown in Fig. 2(a) and 2(b).

[7] A. Sommerfeld, "Die Greensche Funktion der Schwingungsgleichung," *Jahrb. Deut. Math.-Ver.*, Bd. 21, pp. 309–353; March, 1912.

[8] R. Courant and D. Hilbert, "Methoden der Mathematischen Physik I," Julius Springer, Berlin, pp. 302–337; 1931.

[9] K. Fujisawa, "Theory of slotted cylindrical cavities with transverse electric field," *Tech. Reps. Osaka Univ.*, vol. 1, pp. 69–87; March, 1951.

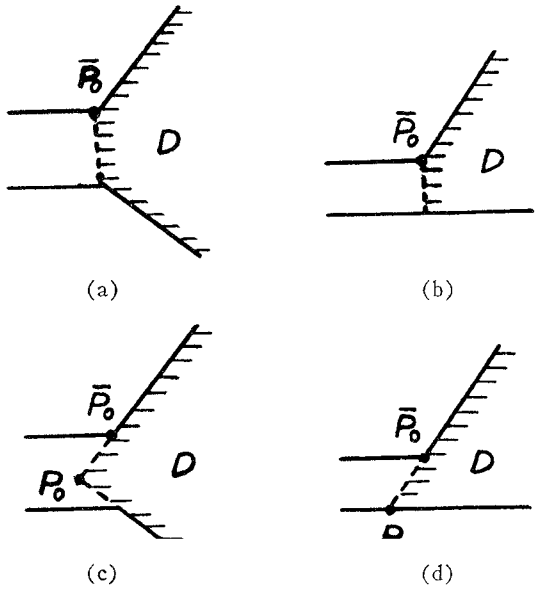

Fig. 2—Determination of the cavity region D. (a) and (b) are unsuitable, and (c) and (d) are suitable, for practical applications.

But for these regions, which have two vertexes on their boundaries at the gaps, it is almost impossible to evaluate the Green's function G. So, for practical applications, it is better to take D as shown in Fig. 2(c) and 2(d), and take the reference point at the vertex P_0 rather than $\bar{P}_0$ to evaluate the Green's function.

Accordingly, we rewrite using (12)

$$\vec{Y}(\bar{P}_0) = 2\pi[u(P_0) - u(\bar{P}_0)] - j\omega\epsilon_0 2\pi \int_{c_0} G(P_0, P'; k^2)\boldsymbol{E}' \cdot d\boldsymbol{s}'. \quad (15)$$

This formula is suitable for practical applications. In the next Section, approximate approaches are given.

General Equivalent Circuit of a Reentrant Cavity

For a reentrant cavity, the resonant wavelength is much greater than the cavity dimensions, so we can put

$$k \ll k_i, \quad i = 1, 2, 3, \cdots. \quad (16)$$

Hence we have, from (11)

$$G(P, P'; k^2) \simeq -\frac{v_0^2}{k^2} + G_1(P, P'), \quad (17)$$

where

$$G_1(P, P') = \sum_{i=1}^{\infty} \frac{v_i(P)v_i(P')}{k_i^2}. \quad (18)$$

Obviously, G_1 is the Green's function for the static

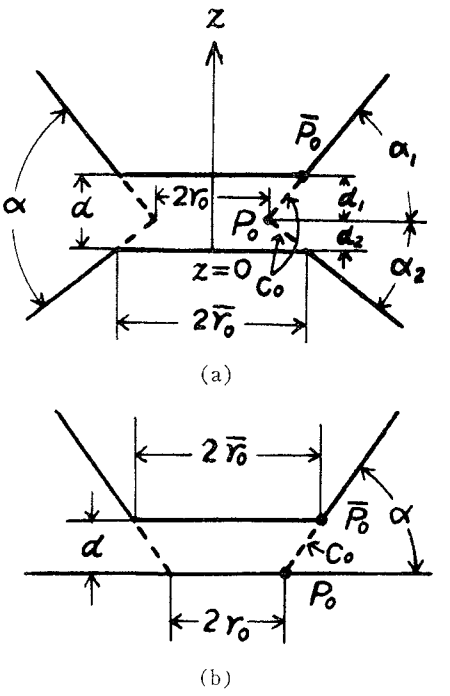

Fig. 3—General shapes of the cavity near the gap.

problem $L'(G_1) = 0$ under the same boundary condition as (5). So, it may be written as

$$G_1(P_0, P') = -\frac{r'}{\alpha} \ln P_0P' + g_1(P_0, P'), \quad (19)$$

where g_1 is a regular function everywhere in D. And it must satisfy

$$\int_D G_1(P_0, P')\frac{dS'}{r'} = 0, \quad (20)$$

by the orthogonality of v_i to v_0 (a constant) in (18). So, substituting (19) in (20), and regarding g_1 as a constant, we can write as

$$G_1(P_0\ P') \simeq -\frac{r'}{\alpha} \ln \frac{P_0P'}{l_M}, \quad \text{for } P_0P' \simeq 0, \quad (21)$$

taking l_M as the mean distance of D to P_0.

Hence, we have finally

$$G(P_0, P'; k^2) \simeq -\frac{1}{k^2 \int_D dS'/r'} - \frac{r'}{\alpha} \ln \frac{P_0P'}{l_M}, \quad \text{for } P_0P' \simeq 0. \quad (22)$$

For the fields in the gap region (Fig. 3), we assume spatially constant electric fields and obtain

$$E_z = \frac{1}{d}, \quad E_r = 0, \quad u = j\omega\epsilon_0 \frac{r^2}{d}. \quad (23)$$

Substituting (22) and (23) in (15), we can write

$$\overrightarrow{Y(P_0)} = \frac{1}{j\omega L} + j\omega C_1, \tag{24}$$

where

$$L = \frac{\mu_0}{2\pi}\int_D \frac{dS'}{r'}, \tag{25}$$

$$\frac{C_1}{\epsilon_0} = \frac{\pi(r_0^2 - \bar{r}_0^2)}{d} + \frac{2\pi}{\alpha d}\left(r_0 d_1 \ln\frac{el_M \sin\alpha_1}{d_1} + \gamma_0 d_2 \ln\frac{el_M \sin\alpha_2}{d_2} + \frac{d_1^2 \cot\alpha_1}{2}\ln\frac{\sqrt{e}l_M \sin\alpha_1}{d_1} + \frac{d_2^2 \cot\alpha_2}{2}\ln\frac{\sqrt{e}l_M \sin\alpha_2}{d_2}\right), \tag{26a}$$

[for the gap shown in Fig. 3(a)],

$$\frac{C_1}{\epsilon_0} = \frac{\pi(r_0^2 - \bar{r}_0^2)}{d} + \frac{2\pi}{\alpha}\left(r_0 \ln\frac{el_M \sin\alpha}{d} + \frac{d\cot\alpha}{2}\ln\frac{\sqrt{e}l_M \sin\alpha}{d}\right), \tag{26b}$$

[for the gap shown in Fig. 3(b)], where $e = 2.718$.

As for the gap capacitance, we assume a gap formed by plane parallel plates instead of the actual gridded gap, and obtain

$$C_0 = \epsilon_0 \frac{\pi\bar{r}_0^2}{d}. \tag{27}$$

If we cannot neglect the effect of grids, the value of C_0 from the above equation should be modified by multiplication by a capacitance reduction factor.

Accordingly, we have, as the total equivalent capacitance of the cavity

$$C = C_0 + C_1. \tag{28}$$

It is very interesting that L, given by (25), is equal to the inductance of a toroidal coil with one turn and with a cross section the same as D. This agrees with the usual empirical statement.[1] But the new introduction of C_1 is found to be very effective.

C_1 is the equivalent capacitance of the cavity region D, and is mainly formed by the capacitance between the side walls of the posts [in Fig. 3(a)], or by that between the side wall of the post and the end plate [in Fig. 3(b)]. It is very interesting to compare the nature of C_1 with those of the usual discontinuity capacitances in transmission lines.

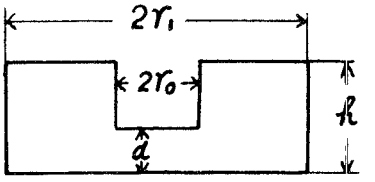

Fig. 4—Reentrant coaxial cavity.

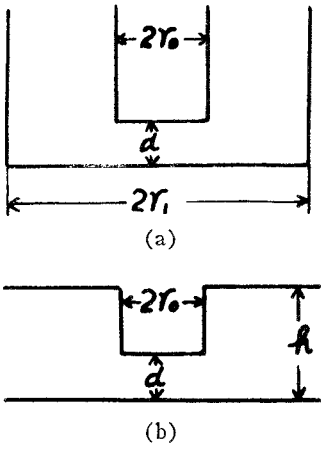

Fig. 5—(a) Coaxial line terminated by a gap; (b) step discontinuity in a radial line.

For this purpose, let us take a reentrant coaxial cavity shown in Fig. 4, for example. In this case, we have

$$C_1 = 4\epsilon_0 r_0 \ln\frac{e\sqrt{(r_1 - r_0)^2 + h^2}}{2d}. \tag{26c}$$

The discontinuity capacitance (excluding the gap capacitance) of the coaxial line terminated by a gap shown in Fig. 5(a), is easily obtained by a little manipulation as[10]

$$C_d = 4\epsilon_0 r_0 \ln\frac{r_1 - r_0}{d}, \quad (r_1 - r_0 \gg d). \tag{29}$$

The step discontinuity capacitance in the radial line shown in Fig. 5(b), is easily obtained as[11]

$$C_d = 4\epsilon_0 r_0 \ln\frac{eh}{4d}, \quad (h \gg d). \tag{30}$$

Comparing the above three capacitances, it is found that C_1 is closely related with the usual discontinuity capacitances in transmission lines, and is slightly greater than

[10] N. Marcuvitz, "Waveguide Handbook," McGraw-Hill Book Co., Inc., New York, N. Y., p. 178; 1951.

[11] C. G. Montgomery, R. H. Dicke, and E. M. Purcell, "Principles of Microwave Circuits," McGraw-Hill Book Co., Inc., New York, N. Y., p. 274, 1948.

these. The difference may be due to the contribution of the electric field in the cavity region far from the gap.

To evaluate C_1 actually, we must know the value of l_M. This is given by

$$l_M = P_0P_M = \frac{1}{S}\int_D P_0P' \cdot dS', \tag{31}$$

taking S as the area of D, and P_M as its center. Also, l_M is obtained graphically by the following procedure.

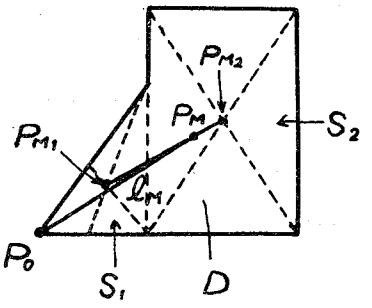

Fig. 6—Graphical determination of l_M.

Given a cavity cross section D as in Fig. 6, for example, we divide it into two regions of simple shapes, and determine the centers of the respective regions, and denote it as P_{M1} and P_{M2}, respectively. Then the center P_M of D is obtained as the dividing point of $P_{M1}P_{M2}$ in inverse proportion to the respective areas, and l_M is found by measuring the distance P_0P_M.

Now, let us turn to the calculation of wall loss. Clearly, the equivalent shunt resistance of the cavity at the gap is given by

$$\frac{1}{R_{sh}} = \int_{c_1} \frac{|2\pi u(P')|^2}{2\pi\delta\sigma}\frac{ds'}{r'}, \tag{32}$$

where σ is the conductivity of the cavity wall and δ is its skin depth.

For a point P' not so close to the gap, we have, from (12) and (13)

$$u(P') \simeq -j\omega\epsilon_0 G(P', P_0; k^2). \tag{33}$$

Substituting (33) in (32), and using (22), we obtain

$$\frac{1}{R_{sh}} \simeq \frac{1}{2\pi\delta\sigma}\frac{1}{\omega^2L^2}\int_{c_1}\frac{ds'}{r'} + \frac{2}{\alpha\delta\sigma}\frac{\epsilon_0}{L}\int_{c_1}\ln\frac{P_0P'}{l_M}ds'$$

$$\simeq \frac{1}{2\pi\delta\sigma}\frac{1}{\omega^2L^2}\int_{c_1}\frac{ds'}{r'}, \tag{34}$$

where we neglected the square of the second term in (22). So, the equivalent series resistance of the cavity at the gap is given by

$$R_{se} = \frac{\omega^2L^2}{R_{sh}} \simeq \frac{1}{2\pi\delta\sigma}\int_{c_1}\frac{ds'}{r'}. \tag{35}$$

Clearly, this is equal to the high-frequency resistance of a toroidal coil with one turn and with a cross section the same as D.

Using these equivalent circuit constants and the equivalent circuits shown in Fig. 7, we can estimate the resonant properties of the reentrant cavities with ease.

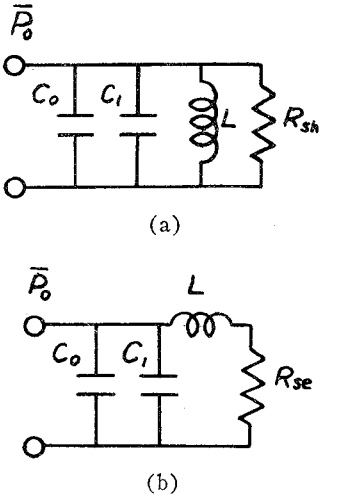

Fig. 7—Equivalent circuits of a reentrant cavity at the gap.

For practical applications, calculated results on typical reentrant cavities are summarized in Table I opposite. The regions of validity of these formulas are discussed in the next Section.

The Ranges of Validity of the Formulas

Generally, the main parameters which affect the validity of the formulas are summarized as the following three:

l_M/λ_0—this shows the relative size of the cavity compared to the resonant wavelength. As referred before, the accuracy is better for smaller l_M/λ_0.

P_0P_V/l_M—taking P_V as the nearest vertex to P_0 on c_1 this affects the validity of (21). The accuracy is better for larger P_0P_V/l_M.

r_0/l_M—this shows the relative size of the post compared to the cavity. The accuracy is better for larger r_0/l_M.

From the following examples, let us now find the ranges of parameters over which the formulas are valid. In Fig. 8 (p. 350) comparisons are made between the calculations from the formulas and those by Hansen, of the resonant wavelengths of the sixty cavities[4] shown in Fig. 9, which, according to his calculations, have the value of $\lambda_0 = 3.2$ cm within an error of 3 per cent. In the figure, the cavities are represented as points in the

TABLE I

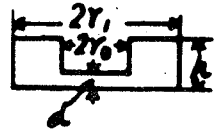 (a)	$\frac{L}{\mu_0} = \frac{h}{2\pi} \ln \frac{r_1}{r_0}, \quad \frac{C_0}{\epsilon_0} = \frac{\pi r_0^2}{d}, \quad \frac{C_1}{\epsilon_0} = 4r_0 \ln \frac{el_M}{d}, \quad l_M = \frac{\sqrt{(r_1 - r_0)^2 + h^2}}{2},$ $\frac{\omega^2 L^2}{R_{sh}} = \frac{1}{2\pi\delta\sigma}\left(\frac{h-d}{r_0} + \frac{h}{r_1} + 2\ln\frac{r_1}{r_0}\right), \quad \lambda = 2\pi\sqrt{r_0 h\left(\frac{r_0}{2d} + \frac{2}{\pi}\ln\frac{el_M}{d}\right)\ln\frac{r_1}{r_0}}$
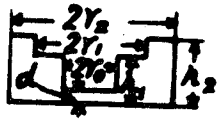 (b)	$\frac{L}{\mu_0} = \frac{1}{2\pi}\left(h_1 \ln\frac{r_1}{r_0} + h_2 \ln\frac{r_2}{r_1}\right), \quad \frac{C_0}{\epsilon_0} = \frac{\pi r_0^2}{d}, \quad \frac{C_1}{\epsilon_0} = 4r_0 \ln\frac{el_M}{d},$ $l_M = \frac{1}{2}\frac{\sqrt{\{(r_1 - r_0)h_1^2 + (r_2 - r_1)h_2^2\}^2 + \{(r_1 - r_0)^2 h_1 + (r_2 - r_1)(r_1 + r_2 - 2r_0)h_2\}^2}}{(r_1 - r_0)h_1 + (r_2 - r_1)h_2},$ $\frac{\omega^2 L^2}{R_{sh}} = \frac{1}{2\pi\delta\sigma}\left(\frac{h_1 - d}{r_0} + \frac{h_2 - h_1}{r_1} + \frac{h_2}{r_2} + 2\ln\frac{r_2}{r_0}\right)$
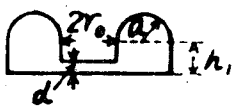 (c)	$\frac{L}{\mu_0} = \frac{1}{2\pi}\left[h_1 \ln\frac{r_0 + 2a}{r_0} + \pi\left(r_0 + a - \sqrt{r_0(r_0 + 2a)}\right)\right], \quad \frac{C_0}{\epsilon_0} = \frac{\pi r_0^2}{d}, \quad \frac{C_1}{\epsilon_0} = 4r_0 \ln\frac{el_M}{d},$ $l_M = \sqrt{a^2 + \left[\frac{h_1}{2} + \left(\frac{4a}{3\pi} + \frac{h_1}{2}\right)\frac{\pi a}{\pi a + 4h_1}\right]^2},$ $\frac{\omega^2 L^2}{R_{sh}} = \frac{1}{2\pi\delta\sigma}\left[\frac{h_1 - d}{r_0} + \frac{h_1}{r_0 + 2a} + \frac{\pi a}{\sqrt{r_0(r_0 + 2a)}} + \ln\frac{r_0 + 2a}{r_0}\right]$
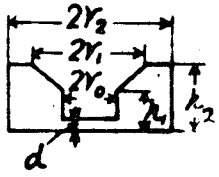 (d)	$\frac{L}{\mu_0} = \frac{1}{2\pi}\left\{\left[h_1 - (h_2 - h_1)\frac{r_0}{r_1 - r_0}\right]\ln\frac{r_1}{r_0} + h_2 \ln\frac{r_2}{r_1} + h_2 - h_1\right\}, \quad \frac{C_0}{\epsilon_0} = \frac{\pi r_0^2}{d}, \quad \frac{C_1}{\epsilon_0} = 4r_0 \ln\frac{el_M}{d},$ $l_M = \frac{1}{3}\frac{\sqrt{\{(r_1 - r_0)(h_1^2 + h_2^2 + h_1 h_2) + 3h_2^2(r_2 - r_1)\}^2 + \{(r_1 - r_0)^2(2h_2 + h_1) + 3h_2(r_2 - r_1)(r_1 + r_2 - 2r_0)\}^2}}{h_1(r_1 - r_0) + h_2(2r_2 - r_1 - r_0)},$ $\frac{\omega^2 L^2}{R_{sh}} = \frac{1}{2\pi\delta\sigma}\left[\frac{h_1 - d}{r_0} + \frac{h_2}{r_2} + \ln\frac{r_2^2}{r_0 r_1} + \frac{\sqrt{(r_1 - r_0)^2 + (h_2 - h_1)^2}}{r_1 - r_0}\ln\frac{r_1}{r_0}\right]$
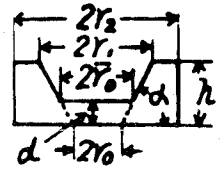 (e)	$\frac{L}{\mu_0} = \frac{h}{2\pi}\left(\ln\frac{er_2}{r_1} - \frac{r_0}{r_1 - r_0}\ln\frac{r_1}{r_0}\right), \quad \frac{C_0}{\epsilon_0} = \frac{\pi\bar{r}_0^2}{d},$ $\frac{C_1}{\epsilon_0} = \frac{\pi(r_0^2 - \bar{r}_0^2)}{d} + \frac{2\pi}{\alpha}\left[r_0 \ln\frac{el_M \sin\alpha}{d} + \frac{d\cot\alpha}{2}\ln\frac{\sqrt{e}l_M \sin\alpha}{d}\right],$ $l_M = \frac{1}{3}\frac{\sqrt{\{2(r_1 - r_0)^2 + 3(r_2 - r_1)(r_1 + r_2 - 2r_0)\}^2 + h^2(3r_2 - 2r_1 - r_0)^2}}{2r_2 - r_1 - r_0},$ $\frac{\omega^2 L^2}{R_{sh}} = \frac{1}{2\pi\delta\sigma}\left(\frac{h}{r_2} + \ln\frac{r_2^2}{\bar{r}_0 r_1} + \sec\alpha \ln\frac{r_1}{\bar{r}_0}\right)$

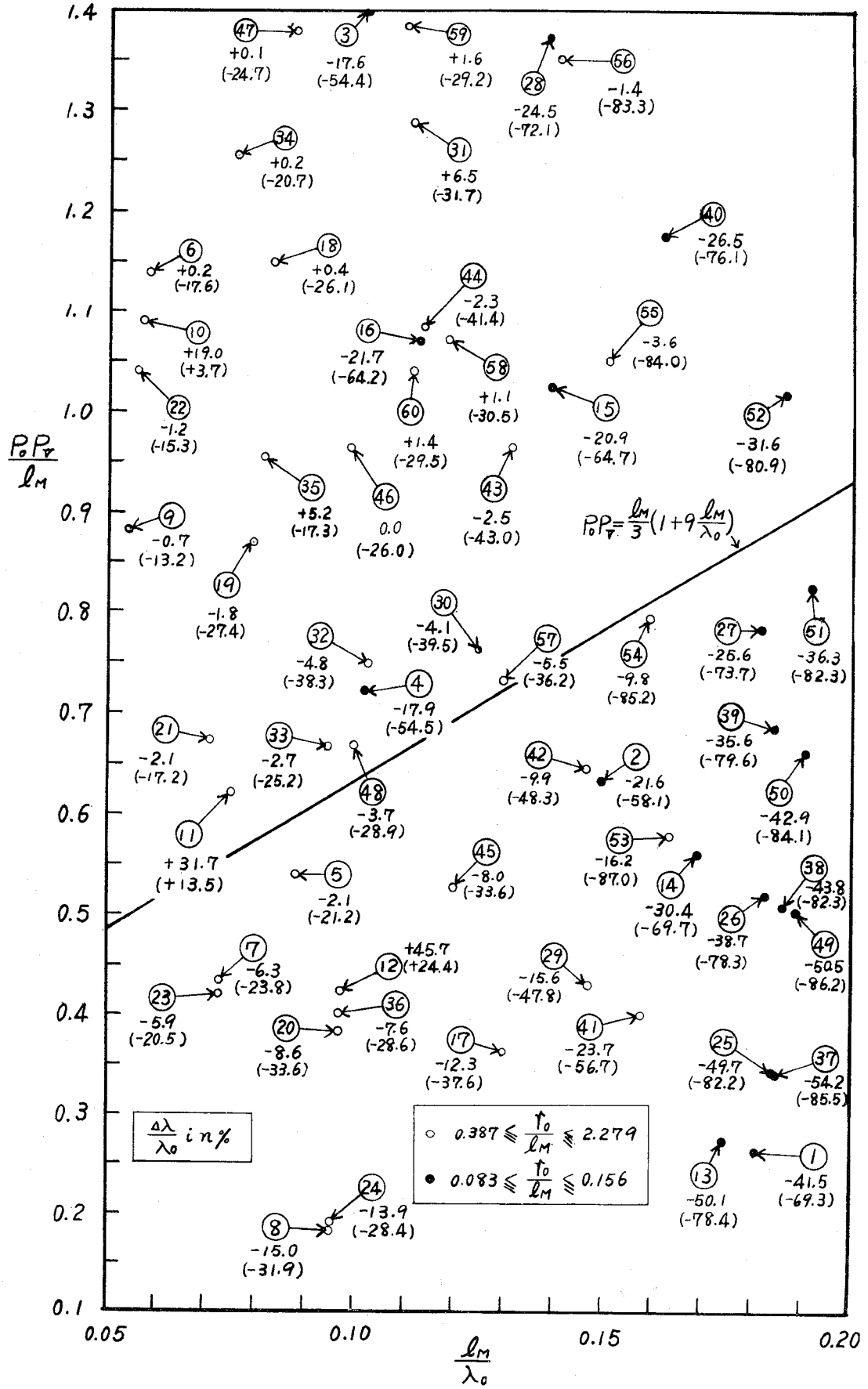

Fig. 8—Percentage differences between the calculations from the formulas and those of Hansen, of the resonant wavelengths of the cavities shown in Fig. 9.

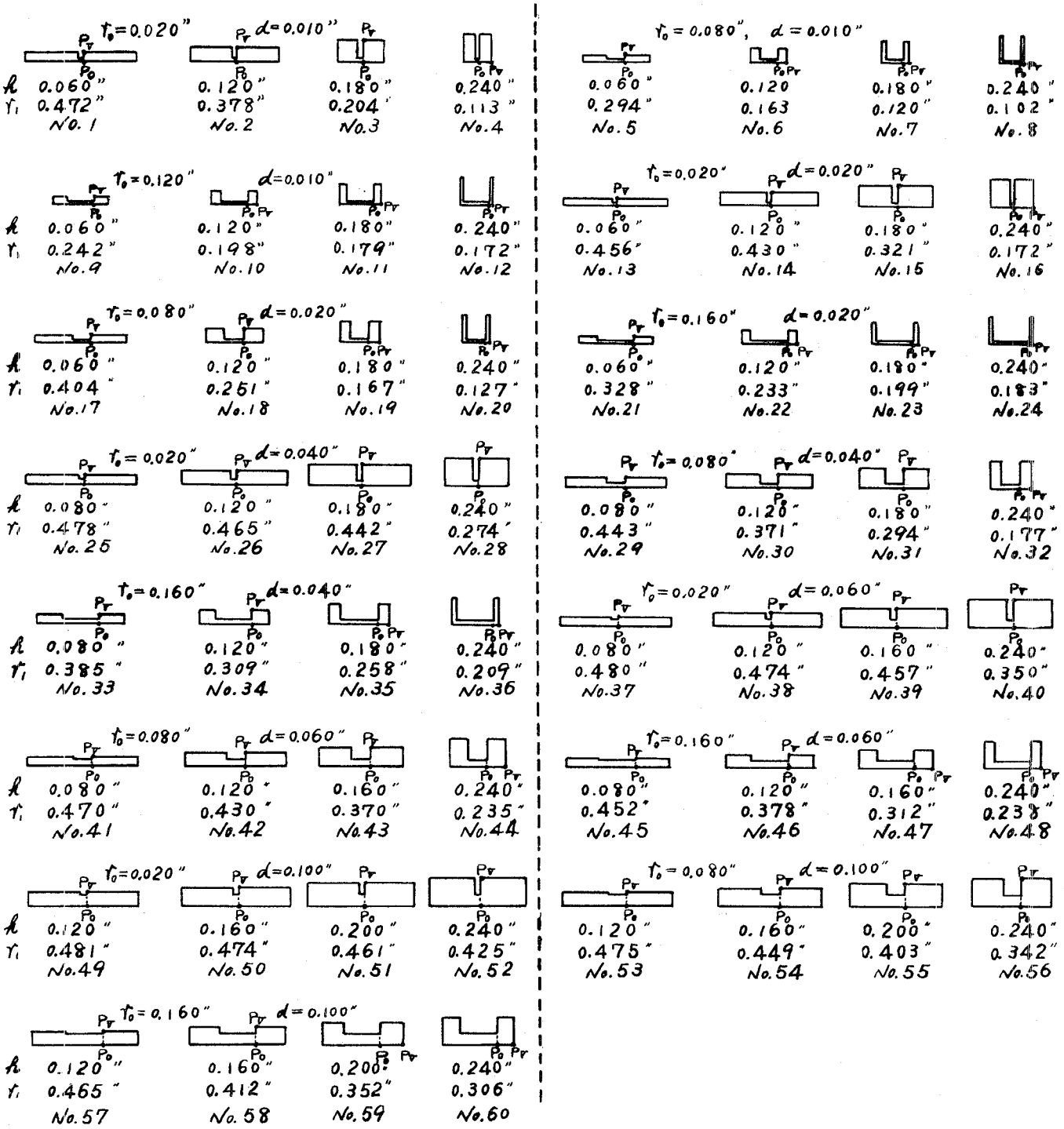

Fig. 9—Reentrant coaxial cavities that have the resonant wavelength of 3.2 cm according to Hansen.

l_M/λ_0-P_0P_V/l_M plane, according to the values of their parameters, and the percentage differences between the two calculations of their resonant wavelengths are indicated. The values in parentheses show the percentage differences between the calculations by the formulas excepting C_1 and those by Hansen.

Clearly, the introduction of C_1 is very effective, and the accuracy is much improved. Also, it is found that the cavities are classified into two groups according to their values of r_0/l_M. For the one group with smaller r_0/l_M($r_0/l_M \leqq 0.156$), the formulas are not applicable, and for the other with larger r_0/l_M($r_0/l_M \geqq 0.387$), they are valid within an error of about 5 per cent, in the region above the straight line indicated in the figure.[12]

[12] Three cavities, Nos. 10, 11 and 12, show extraordinarily great and unusually directed errors. Since some misprints probably may be included in Hamilton, Knipp, and Kuper, *op. cit.*, these three cavities are to be omitted.

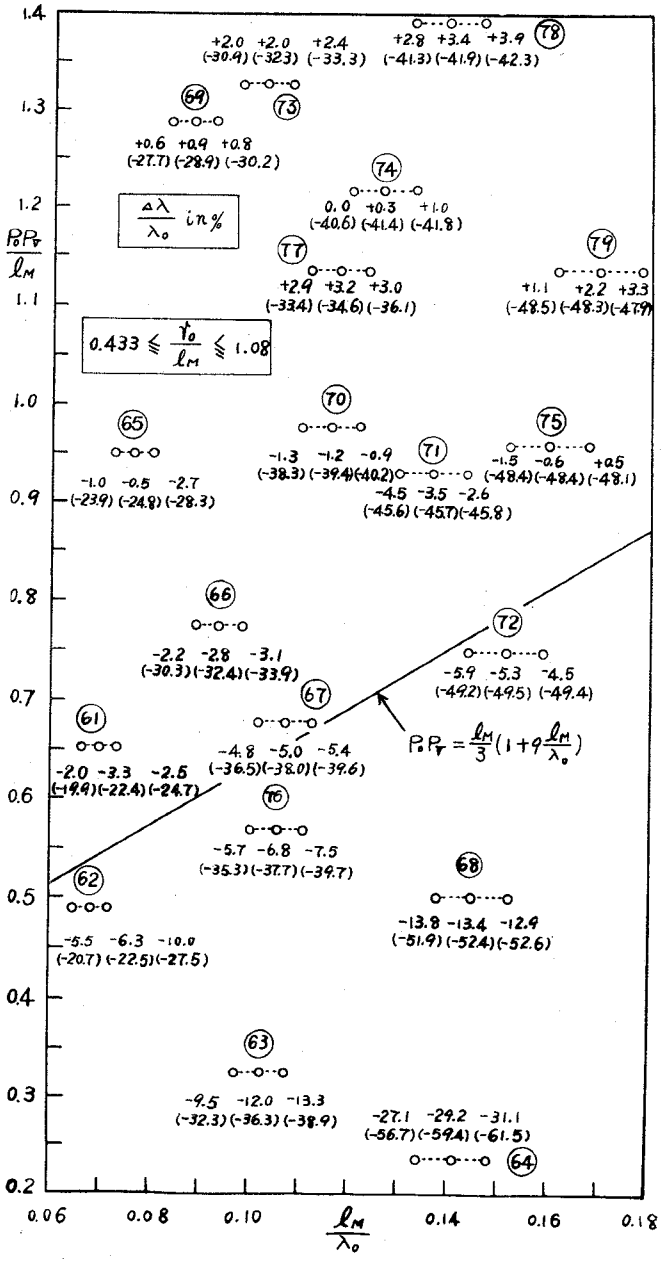

Fig. 10—Percentage errors of the calculated resonant wavelengths of the cavities shown in Fig. 13.

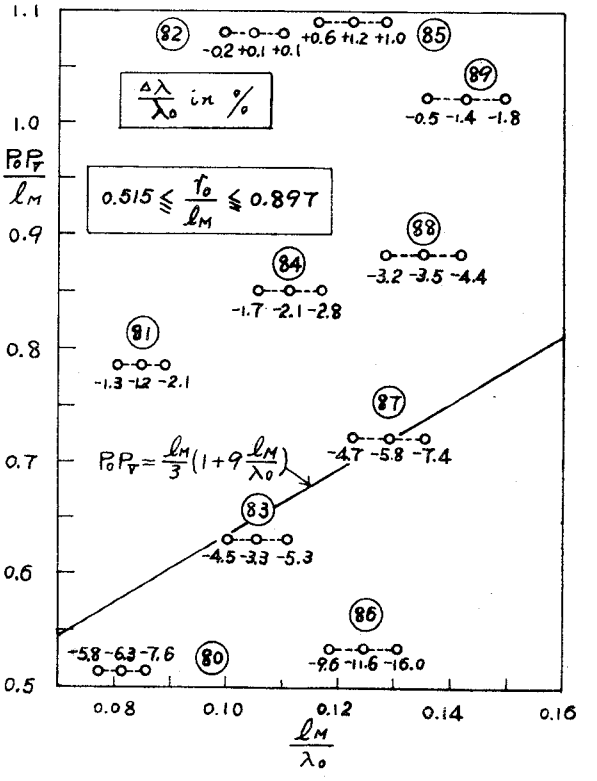

Fig. 11—Percentage errors of the calculated resonant wavelengths of the cavities shown in Fig. 14.

In Figs. 10–12, the calculated resonant wavelengths obtained by the formulas are compared with results of the experiments of the cavities (Figs. 13–15, pp. 354–355), and their percentage errors are given. These cavities all have the resonant frequencies of 3800, 4000, and 4200 mc at the gap distances indicated (the smaller gap distance corresponds to the lower resonant frequency). The values in parentheses in Fig. 10 show the percentage errors of the calculated resonant wavelengths by the formulas excepting C_1.

Here also the effectiveness of C_1 is proved. Fig. 17 shows the percentage errors of the calculated resonant wavelengths compared with results of experiments of the cavities[13] shown in Fig. 16. In these cases, the resonant wavelengths are varied from about 13 cm to about 32 cm.

The experimental values of the resonant wavelengths are affected by the external loads through the loop coupling, so they contain some errors probably smaller than a few per cent.

From these figures, it is concluded that the introduction of C_1 is very effective, and the resonant frequency may be calculated by the formulas to within an error of about 5 per cent in the following ranges of parameters:

$$r_0/l_M \geqq 1/3, \tag{36}$$

and

$$P_0P_V/l_M \geqq 1/3 + 3l_M/\lambda_0. \tag{37}$$

This condition applies for the case when the boundary c_1 subtends a right angle at the vertex P_V. If the angle at P_V is larger than a right angle, the bend at P_V affects the validity of (21) less, so that the formulas are applicable to smaller values of P_0P_V/l_M than are given by (37). This is understood from the data of the cavities Nos. 110 and 111 in Fig. 17.

As for the shunt resistance and the unloaded Q, comparisons were made between the values of the formulas

[13] The cavities Nos. 108 and 109 are the doubly-scaled cavity models of the klystron 2K56 and 2K54.

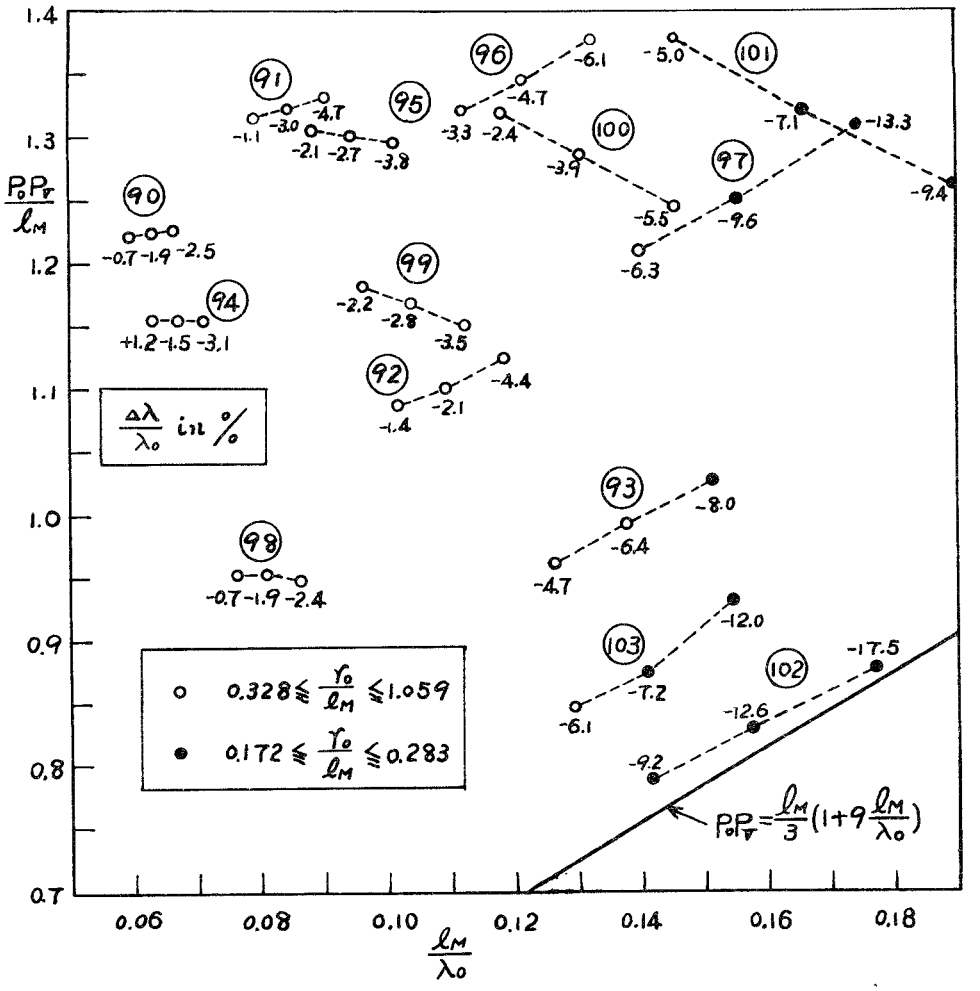

Fig. 12—Percentage errors of the calculated resonant wavelengths of the cavities shown in Fig. 15.

and those of Hansen, for the sixty cavities shown in Fig. 9. The percentage differences between the two calculations are smaller than about 50 per cent,[14] but their values distribute irregularly and it seems impossible to find any rules for the resonant frequency. This may be due to the fact that both calculations contain considerable errors,[15] and we have no standard values to compare them with.

Also, the shunt impedance R_{sh}/Q_0 of the reentrant coaxial cavity with a square cross section was calculated by the formulas and compared with the results of Ginzton and Nalos.[16]

The values according to the formulas are in close agreement with their calculated values based on a mean value between coaxial and radial field approximation, and are accurate to 15 per cent for values of kr_0 up to 0.6 provided that $kd<0.5$.

From the above discussions, it is concluded that the formulas may give the shunt resistance and the unloaded Q to within an error of several tens of per cent in most cases.

Special Cases

Case 1—A Reentrant Cavity with a Gridless Gap

So far, we have considered only reentrant cavities with a gridded gap. But, for high power and for extremely high frequency, one uses klystrons with a gridless gap. In Fig. 18, such a gap is shown, which is formed by a cylinder of inner radius $\bar{r}_i$ and outer radius $\bar{r}_0$ and an end plate with an aperture of radius $\bar{r}_a$, at a distance d apart. We assume here that the end plate has a thickness greater than the aperture radius, so that the aperture behaves as a cylinder for the gap fields. The gap fields excite a cutoff E-type mode with axial symmetry in the cylinders.

Such a problem was solved in detail by Wang.[17]

[14] Here also the cavities Nos. 10, 11 and 12 were omitted.

[15] The calculations by W. W. Hansen of the shunt resistance and the Q are believed to be accurate to 10 per cent for cavities highly reentrant and to 25 per cent for those that are less so.

[16] Ginzton and Nalos, *op. cit.*, p. 5, Fig. 5.

[17] C. C. Wang, "Electromagnetic field inside a cylinder with a gap," *J. Appl. Phys.*, vol. 16, pp. 351–366; June, 1945.

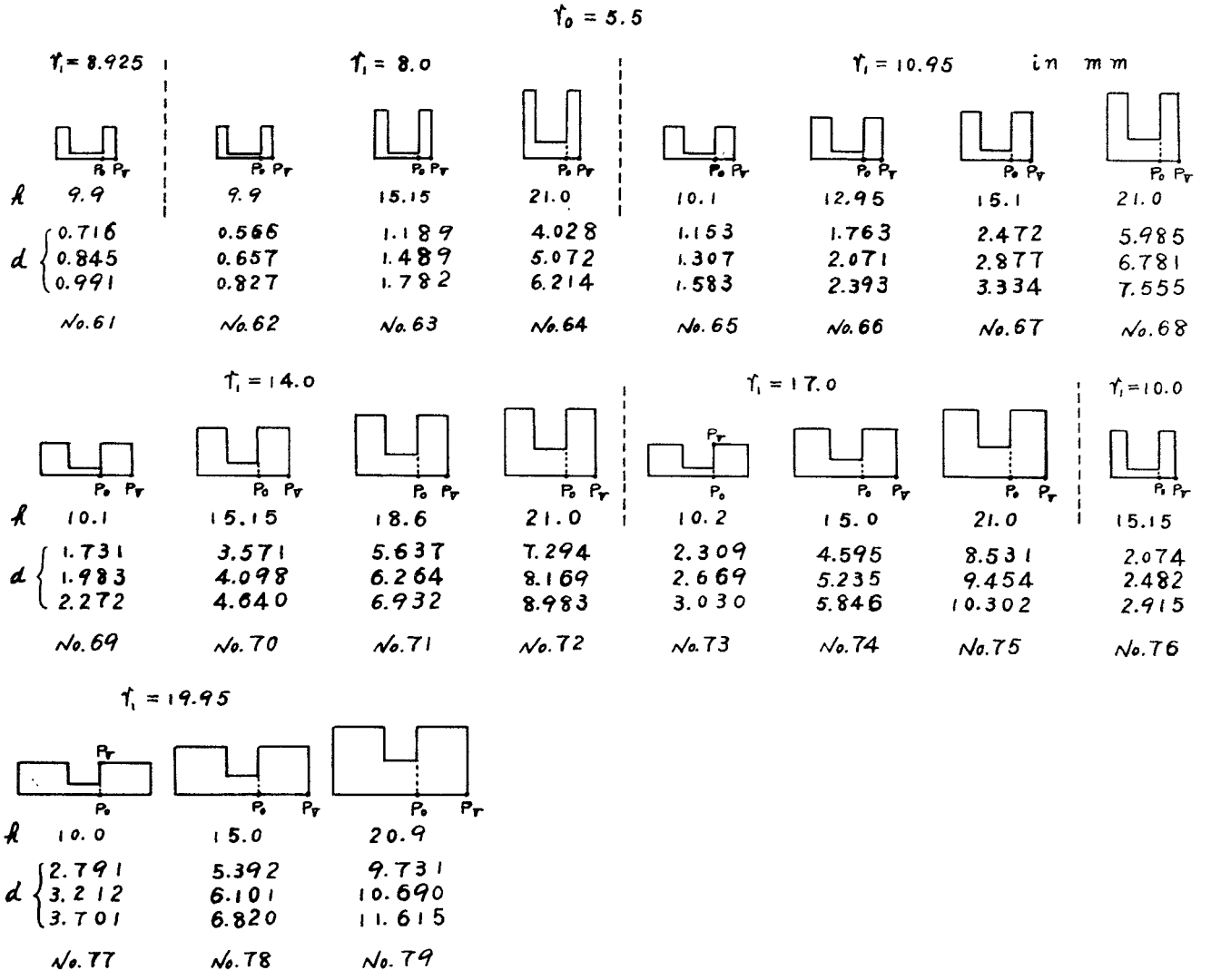

Fig. 13—Reentrant coaxial cavities that have the resonant frequencies of 3800, 4000, and 4200 mc experimentally.

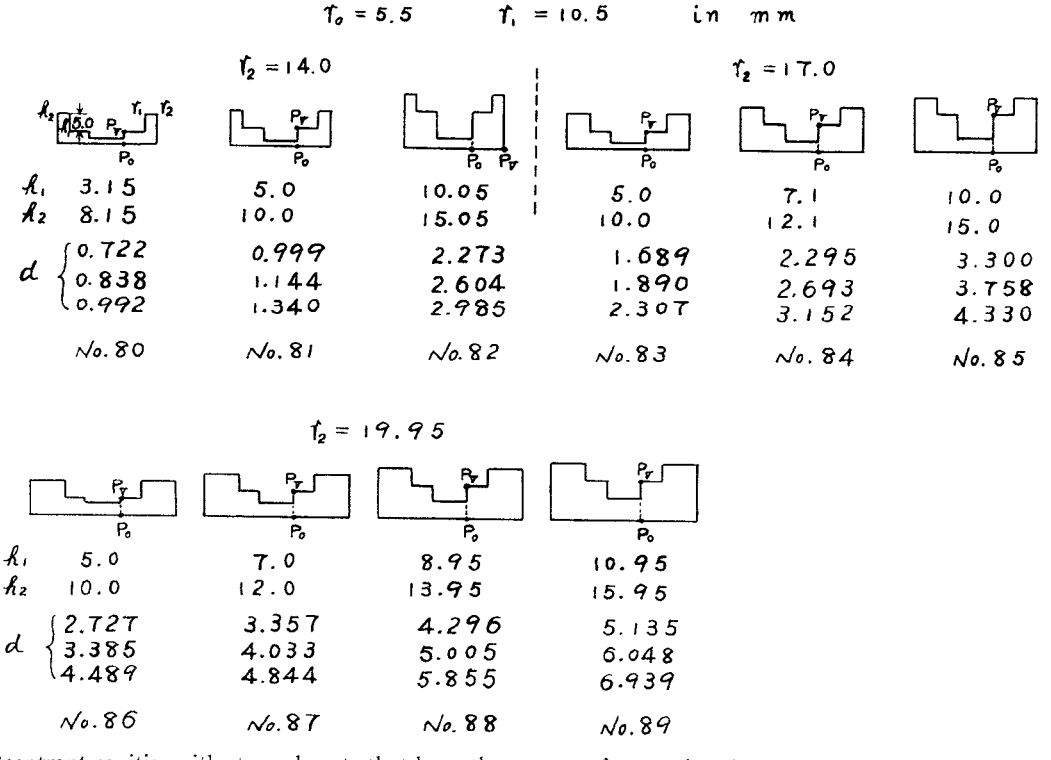

Fig. 14—Reentrant cavities with stepped posts that have the resonant frequencies of 3800, 4000, and 4200 mc experimentally

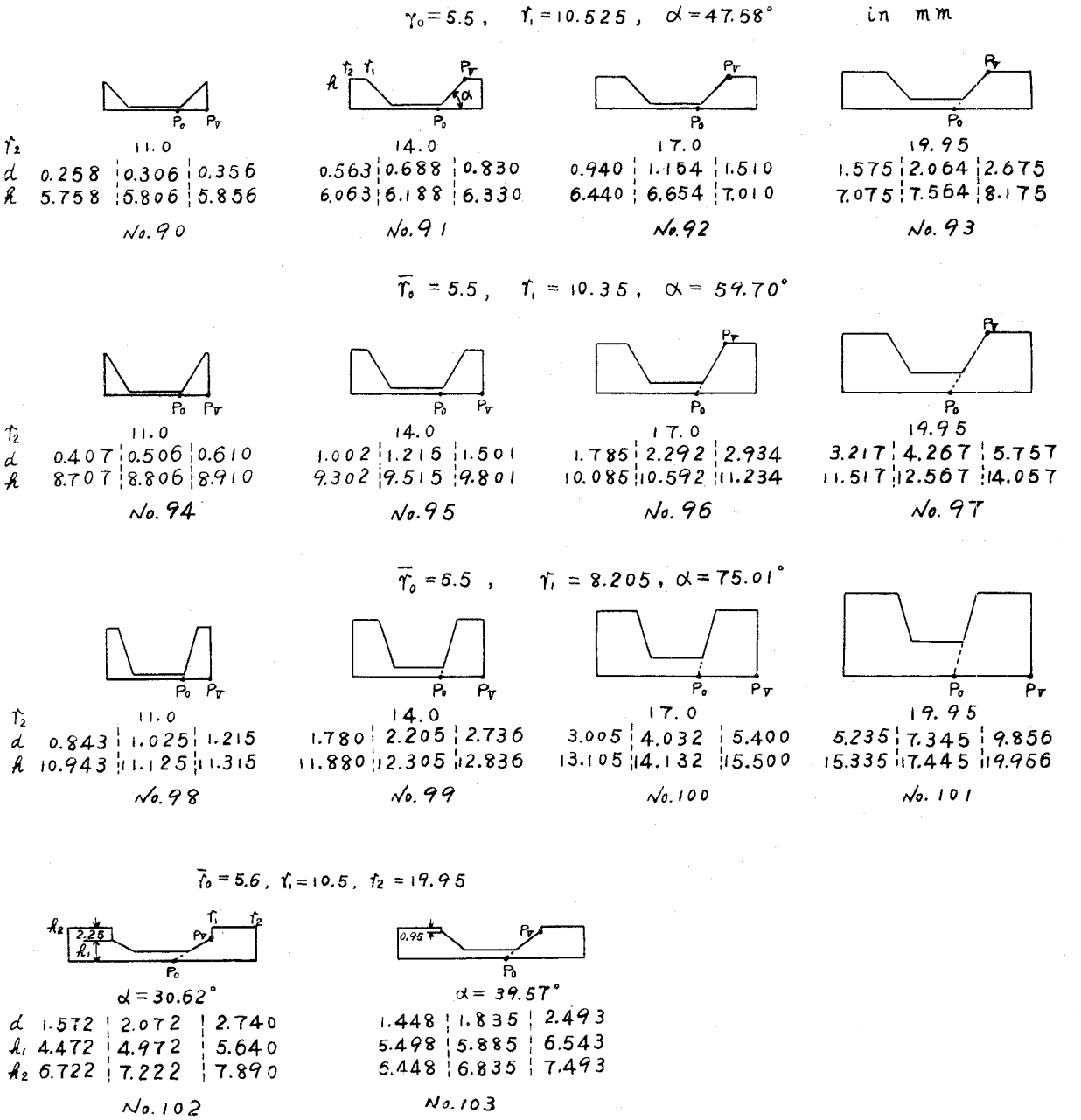

Fig. 15—Reentrant cavities that have the resonant frequencies of 3800, 4000, and 4200 mc experimentally.

Later, it was treated by the author independently, and the following results are derived.[18]

Assuming a space constant electric field on the cylindrical surface $r=\bar{r}_i$ in the gap region, and expressing the fields in Fourier integrals of the elementary waves in the cylinders, the equivalent gap capacitance C_0 is obtained as

$$C_0 = \epsilon_0 \frac{\pi(\bar{r}_0^2 - \bar{r}_i^2)}{d} + \epsilon_0 \frac{\pi \bar{r}_i^2}{d} \gamma\left(\frac{d}{\bar{r}_i}, k\bar{r}_i\right). \qquad (38)$$

Clearly, γ is a capacitance reduction factor for the gridless gap as compared with the gridded one, and its values are given in Fig. 19, p. 357.

[18] K. Fujisawa, "Gridless modulation gap of a klystron," *J. Inst. Elec. Comm. Eng. Japan*, vol. 36, pp. 613–617; November, 1953.

Substituting (38) for (27), all the former relations remain valid in the same ranges of parameters given by (36) and (37).

Case 2—A Reentrant Cavity with a Post Stepped near the Tip

Such a cavity is shown in Fig. 20. By taking the cavity cross section D as shown in Fig. 20(a), as usual, we sometimes have more small values of P_0P_V/l_M than are given by (37), and cannot apply the formulas. In such cases, by taking D as shown in Fig. 20(b), the conditions (36) and (37) are often satisfied, and the formulas become applicable in certain conditions.

In Fig. 20(b), the equivalent gap capacitance consists of the capacitances of the plane parallel plates of the circular and annular areas and the discontinuity capacitance at $r=r_0$ given by (30). So it is written as

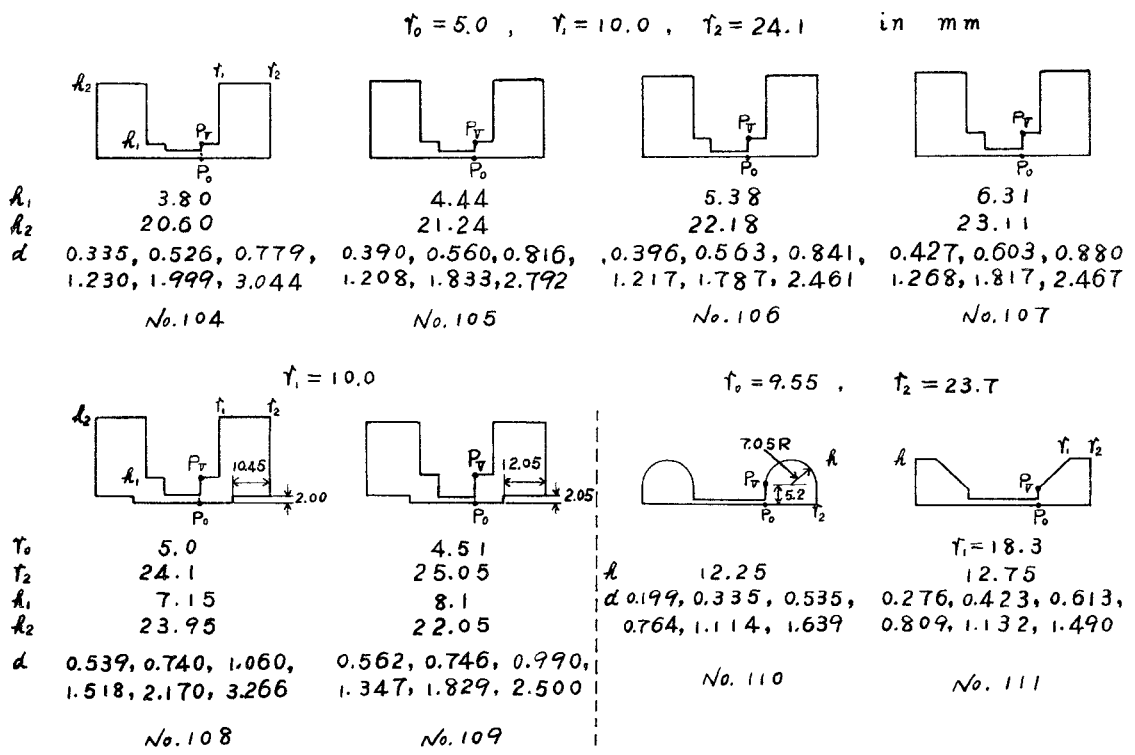

Fig. 16—Various reentrant cavities that have the resonant wavelengths between 13 cm and 32 cm.

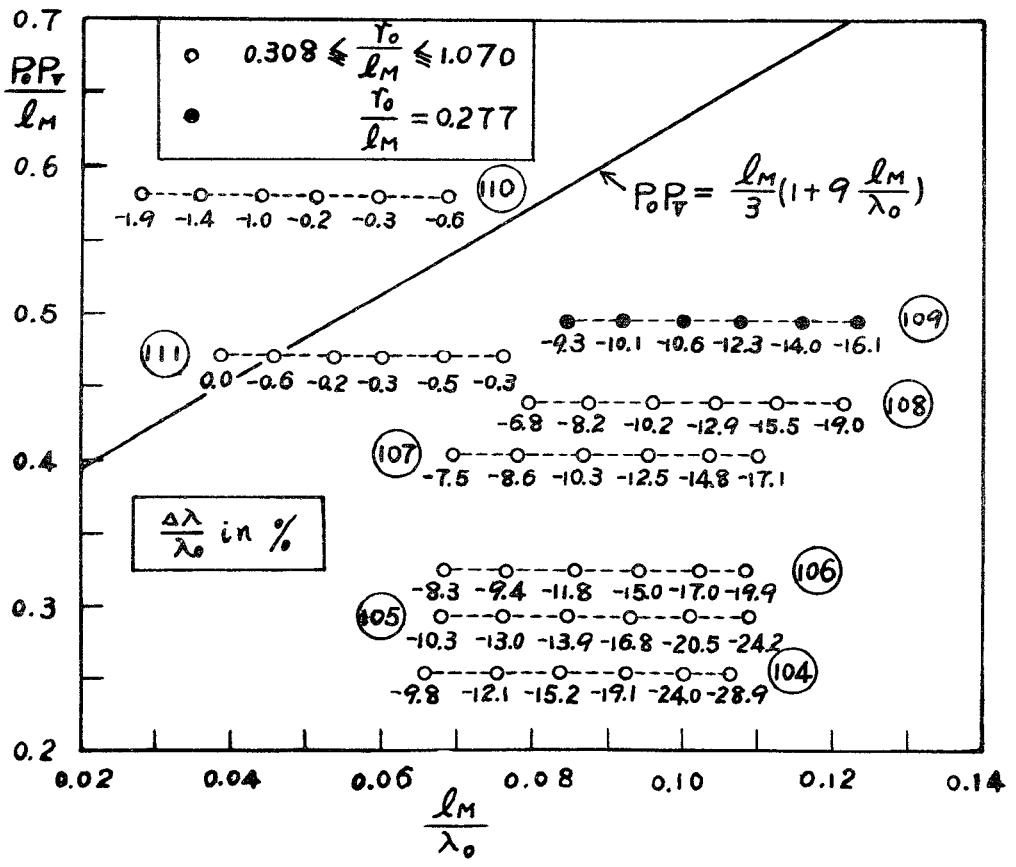

Fig. 17—Percentage errors of the calculated resonant wavelengths of the cavities shown in Fig. 16.

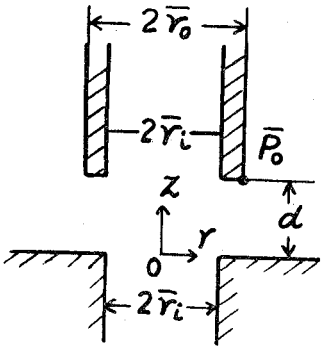

Fig. 18—Typical gridless gap.

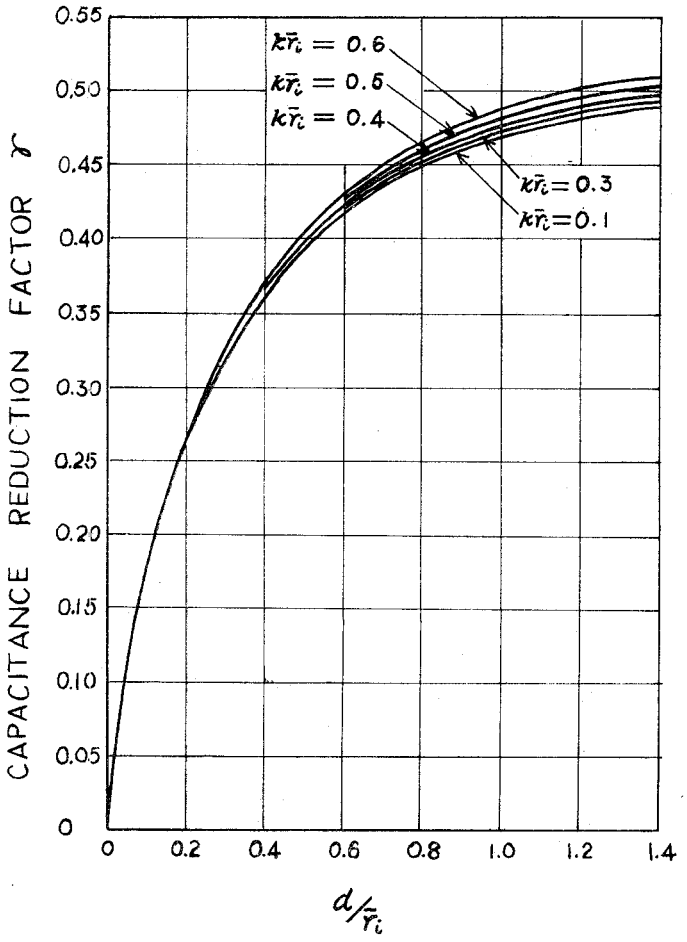

Fig. 19—Capacitance reduction factor for the gridless gap as compared with the gridded one.

$$C_0 = \epsilon_0 \frac{\pi r_0^2}{d} + \epsilon_0 \frac{\pi(r_1^2 - r_0^2)}{h_1} + 4\epsilon_0 r_0 \ln \frac{eh_1}{4d} \cdot \quad (39)$$

Substituting (39) for (27), all the resonance properties are calculable.

By this method, the resonant wavelengths of several cavities were calculated, and their percentage errors compared with experiments are given in Fig. 21 (p. 358). Formerly, these cavities were treated by taking D as usual, and the percentage errors of their calculated resonant wavelengths are given in Figs. 11 and 17. Comparing these data, it is concluded that by this method some cavities are brought into the applicable regions of the formulas [(36) and (37) are satisfied], and their resonant frequencies are calculable within an error of 5 per cent, when the following additional condition is satisfied for the new cavity region D:

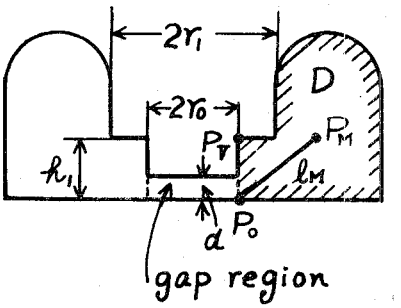

(a)

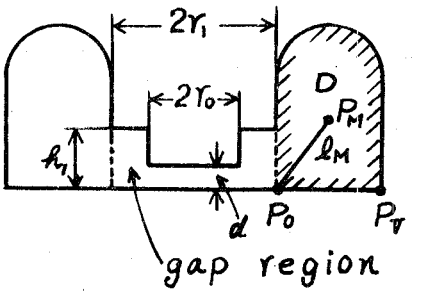

(b)

Fig. 20—Two methods of taking the cavity region D for a cavity with a stepped post.

$$\frac{d}{h_1} \geqq \frac{4}{5}\left(\frac{h_1}{l_M} - \frac{1}{5}\right). \quad (40)$$

Conclusion

In this paper, general formulas for calculating the equivalent circuit constants of a reentrant cavity are derived, which enable one to calculate the resonant frequency within an error of 5 per cent, in the ranges of parameters given by (36) and (37), and the shunt resistance and the Q within an error of several tens of per cent in most cases. For practical klystron cavities, the conditions (36) and (37) are usually satisfied, so that the formulas are applicable for most klystron cavities.

Acknowledgment

This work was carried out partly at Osaka University, and partly at Kobe University following the author's transfer to Kobe University in 1954.

The author expresses his sincere thanks to Prof. S. Kumagai for his support and encouragement at Osaka University. He also wishes to acknowledge the valuable assistance of T. Yuwamoto and S. Otsuka at Osaka University and of T. Kaneko and T. Takashima at Kobe University.

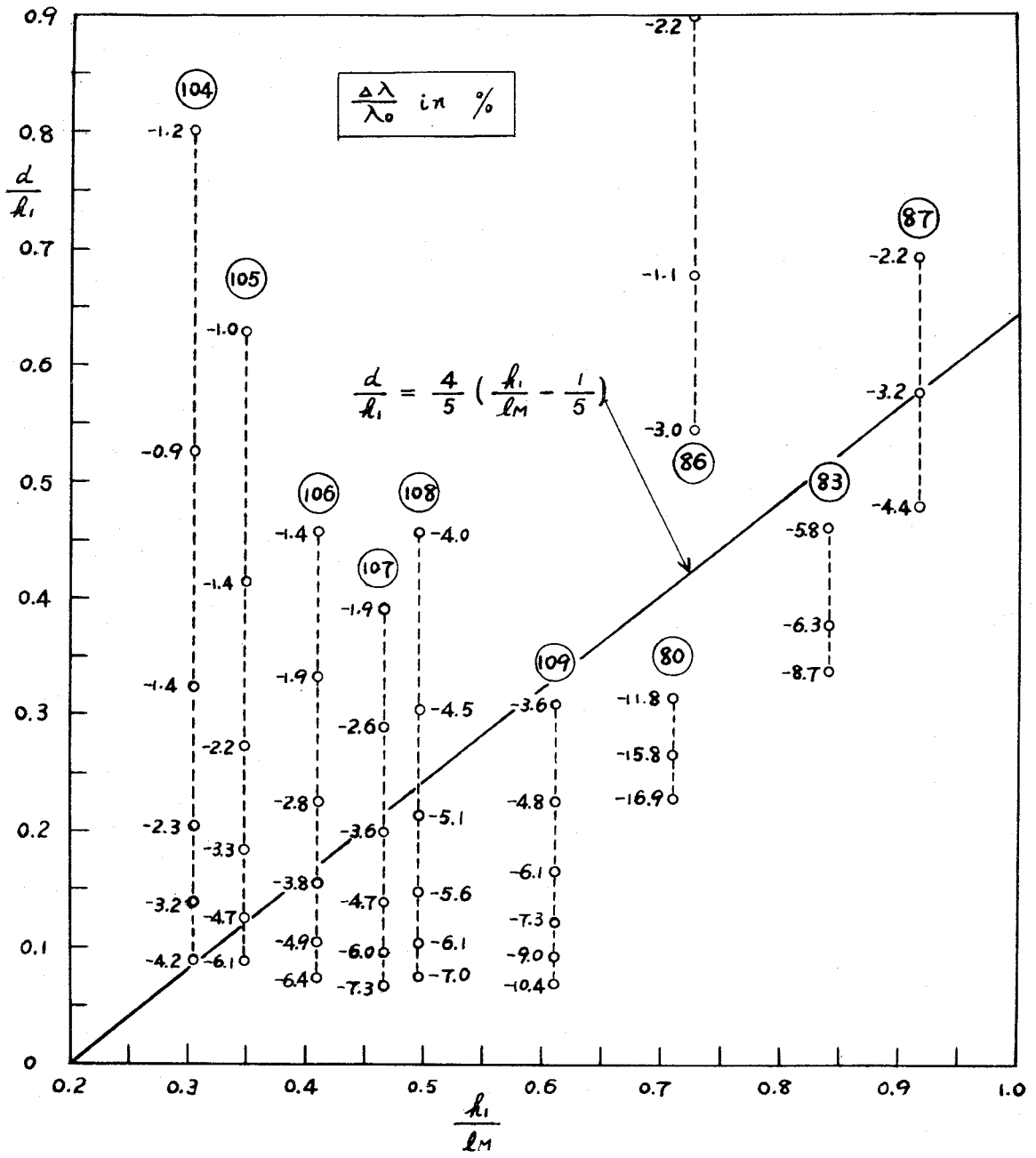

Fig. 21—Percentage errors of the resonant wavelengths calculated by taking D as in Fig. 20(b).